Hindawi Publishing Corporation
International Journal of Plasma Science and Engineering
Volume 2008, Article ID 284549, 5 pages
doi:10.1155/2008/284549

Research Article

FFT Analysis of a Series Loaded Resonant Converter-Based Power Supply for Pulsed Power Applications

R. B. Jadeja,[1] S. A. Kanitkar,[2] and Anurag Shyam[3]

[1] *Department of Electrical and Electronics Engineering, C.U. Shah College of Engineering and Technology, Wadhwan City-363030, Gujarat, India*
[2] *Department of Electrical Engineering, Maharaja Sayajirao University of Baroda (M.S.), Vadodara, 390006 Gujarat, India*
[3] *Pulsed Power Group, Pulsed Power Laboratory, Institute of Plasma Research, Gandhinagar, 382428 Gujarat, India*

Correspondence should be addressed to R. B. Jadeja, rbjadeja2001@ccetvbt.org

Received 20 June 2007; Revised 22 November 2007; Accepted 18 February 2008

Recommended by Andrew Christlieb

An impulse power supply has been designed, simulated, and tested in order to feed the primary of a high-frequency transformer. Pulse power system has been widely used for plasma applications. The operational principle of the pulse power system is that the energy from the input source is stored in the capacitor bank device through a dc-dc converter. Then, when a discharging signal is given, the stored energy is released to the load. The new family of ZCS converters is suitable for high-power applications using insulated gate bipolar transistors (IGBTs). The power converter can achieve zero switching with the aid of high-frequency transformer. The device is capable of charging a 0.1 μF capacitor up to 5 kV which accounts for a charging power of 5 kJ/s. The novel control algorithm is achieved which eminently considers the nonlinear control characteristics of impulse power supply. The required charging voltage, together with the constraint on the charging time, translates into a required maximum power of 10 kW reduced in this initial version to 5 kW. The difficulty to reliably control such a power at the high-voltage side practically forbids any approach featuring a more or less stabilized DC high-voltage to be generated from a conventional 50 Hz transformer through rectification.

1. INTRODUCTION

For many years, power electronics in the high-power area was performed with slow semiconductor switches like MOSFET and BJT. The IGBT is a relatively new power semiconductor device, which provides the best features of both the MOSFET and the BJT [1]. Its advantages are low power, voltage-driven turn on and turn off, gate impedance as high as MOSFET, low-conduction losses, and positive temperature coefficient. The device will not experience thermal run-away as of BJTs. Possibility to use either integrated or external antiparallel diode. Recent improvements in high-power semiconductor technology have given switching performance similar to that of the IGBTs to the high-power area through the advancement of the IGBTs. This paper explains the internal dynamics [2] of IGBT behavior in zero current switching circuit topologies. The impulse power supply described in this paper has been initially built to provide a charging power of 5 KW only. The impulse power supply differs from conventional power supply in that capacitor charging requires operation over a wide range of load conditions varying from nearly short circuit, when the capacitor has no charge, to nearly open circuit, when the capacitor is almost fully charged. This kind of performance can be best achieved by supplying a constant charging current. The instantaneous output power then is minimum at the charge beginning and maximum at the charge end. The paper proposes a novel topological circuit of stable voltage source power converter using latest IGBTs (IRG4PH40PUD).

2. SYSTEM DESIGN

The required charging voltage, together with the constraint of the charging time, translates into a required maximum power of 10 KW reduced in this initial version to 5 KW as shown in Figure 1. The difficulty to reliably control such a power at the high-voltage side practically forbids any approach featuring a more or less stabilized DC high-voltage

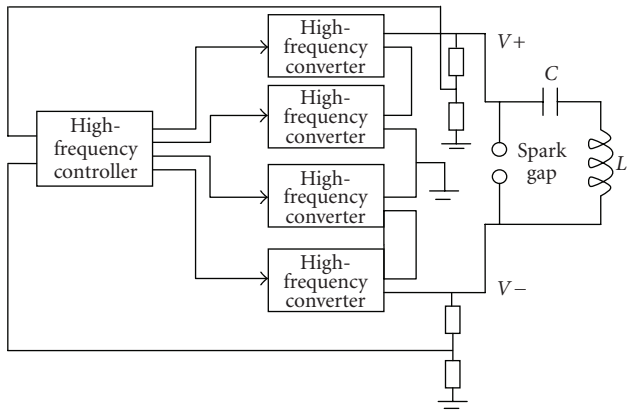

Figure 1: Power supply architecture.

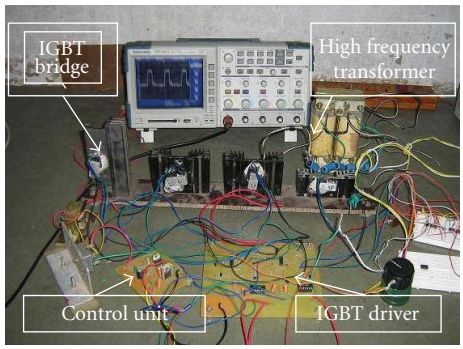

Figure 2: Hardware testing.

to be generated from a conventional 50 Hz transformer through rectification, as shown in Figure 2.

Instead, it is more attractive to utilize a high-frequency converter performing the regulation at the low-voltage side of its step-up transformer and charging the primary capacitor with high-voltage pulses. Such a device is not capable of providing a stabilized DC voltage and, therefore, can be merely regarded as an impulse power supply. The modular architecture allows simplifying the problem of the construction of the 20 KV, 5 KW step-up transformers and the selection of electronic components suitable to drive it. A subdivision of the power supply into four identical blocks reduces the requirements to four 5 KV, 1.25 KW modules, which can be implemented with off-the-shelf components.

The design is scalable, as more converter modules can be added in series to reach a higher charging voltage, with their output floating respect to ground. The capacitor charging power supply (CCPS) output is internally center-tapped to ground one of the output leads. Hence it assumes a maximum potential of +10 KV while the other one assumes a minimum potential of −10 KV (respect to ground). This strategy increases safety and allows reducing to one half (10 KV DC) the insulation requirement of assemblies and wiring. A single controller module samples the charging voltage and drives the converter. It is responsible for synchronizing the charge with external events and suspending the charging pulses when a predetermined voltage is reached. Galvanic isolation at several points is either required or desirable in order to reduce noise and interference.

3. HIGH-FREQUENCY CONVERTER

The basic block diagram of one converter module as shown in Figure 3. The converter modules are fed with 560 V DC obtained by rectifying 400 V AC from the mains. A full-bridge switch drives a step-up transformer with a 9 : 1 turns ratio in order to reach a rectified output voltage of about 5 KV DC. The switch commutation is externally driven by the controller (UC3860) module, according to the capacitor charge state as shown in Figure 4.

The topology selected for the converter is the series-loaded resonant (SLR) [3, 4]. In this configuration, the switches and resonant components L and C are connected to the low-voltage side of the transformer. Only the rectifiers on the transformer secondary must have high-voltage ratings. By closing, in proper order, the switches in pairs, pulses of alternate polarity are applied to the transformer using a high-turn ratio, high-voltage pulses are generated at the secondary, increasing the capacitor charge.

4. THEORY OF OPERATION

The characteristic impedance Z_0 of the bridge load is given by

$$Z_0 = \sqrt{\frac{L}{C_{\text{eq}}}}. \tag{1}$$

And its resonance frequency f_0 is given by

$$f_0 = \frac{1}{2\pi\sqrt{LC_{\text{eq}}}}, \tag{2}$$

C_{eq} is the series combination of capacitors C and C_c', where C_c' is the equivalent capacitance C_c reflected in the primary [5–8]

$$C_c' = \left(\frac{N_2}{N_1}\right)^2 C_c = 81 \cdot C_c. \tag{3}$$

Usually in high-voltage applications, C_c (0.1 μF in our case) is at least order of magnitude greater than C. While its contribution is negligible:

$$C_{\text{eq}} = \frac{1}{1/C + 1/C_c'} \approx C. \tag{4}$$

Therefore, Z_0 and f_0 are uniquely defined by C and L. Operating the circuit at a frequency $f_s < f_0/2$, all switches and antiparallel diodes turn on and off at zero current. Using a frequency $f_0/2 < f_s < f_0$, the diodes turn off and the switches turn on happen at a current greater than zero. Conversely, for $f_s > f_0$, the diodes turn on and the switches turn off at a current greater than zero [9].

5. RESULTS

The maximum peak reverse current flowing through the diodes when one switch pair is open is given by

$$I_{\text{OFF max}} = \frac{V_{\text{in}}}{Z_0}. \tag{5}$$

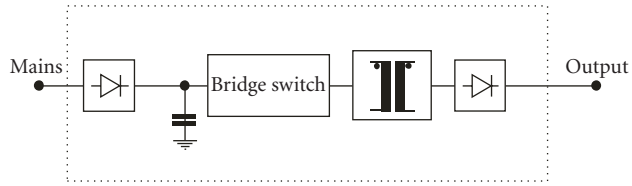

Figure 3: Basic block diagram of one converter module.

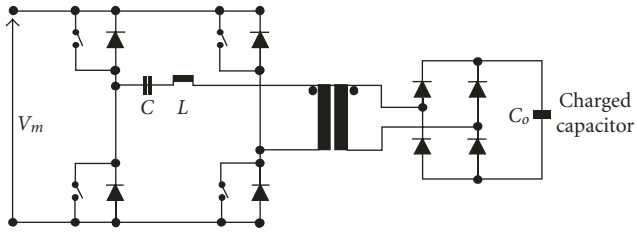

Figure 4: Schematic diagram of the high-frequency converter.

The above value is assumed at the beginning of charging and drops down to zero at the end of charge. This is due to the voltage reversal effect across the load terminals, caused by the voltage present on the capacitor under charge. Conversely, the maximum peak current flowing in the load C2 and L1 when a switch pair is closed is given by

$$I_{\mathrm{ON\,max}} = \frac{2V_{\mathrm{in}}}{Z_0} = -2I_{\mathrm{OFF\,max}}. \tag{6}$$

This value is reached only at the end of the charge and is due to the energy accumulated in the resonant load C2 and L1 at charge beginning is $I_{\mathrm{ON}} = -I_{\mathrm{OFF\,max}}$. Therefore, the SLR converter switches must be capable to stand $I_{\mathrm{ON\,max}}$, while the diodes can be sized to operate at $I_{\mathrm{OFF\,max}}$ only:

$$\begin{aligned} I_{\mathrm{OFF\,max}} &= -\frac{V_{\mathrm{in}}}{Z_0} = -\frac{V_{\mathrm{in}}}{\sqrt{L_1/C_2}} \\ &= \frac{-560}{\sqrt{0.07\times10^{-3}/0.037\times10^{-6}}} = -13\,\mathrm{A}, \\ I_{\mathrm{ON\,max}} &= -2I_{\mathrm{OFF\,max}}. \end{aligned} \tag{7}$$

The RMS capacitor charging current can be calculated directly from the capacitor charging rate. Where ΔV is the difference between output and input of the transformer:

$$I_{\mathrm{Crms}} = \frac{C_1\Delta V}{\Delta t} = \frac{0.1\times10^{-6}\times5000}{600\times10^{-6}} = 832\,\mathrm{mA}. \tag{8}$$

The RMS current in the resonant load and transformer primary $I_{1\,\mathrm{rms}}$can be calculated by balancing the average power between capacitor (P_{Cave}) and load (P_{Lave}):

$$P_{\mathrm{Cave}} = \frac{I_{\mathrm{Crms}}\cdot\Delta V}{2} = \frac{832\times10^{-3}\times5000}{2} = 2080\,\mathrm{W}, \tag{9}$$

$$I_{1\mathrm{rms}} = \frac{P_{\mathrm{Lave}}}{V_{\mathrm{in}}} = \frac{P_{\mathrm{Cave}}}{V_{\mathrm{in}}} = \frac{2080}{560} = 3.714\,\mathrm{A}, \tag{10}$$

$$\begin{aligned} P &= \frac{0.5\cdot C_1\cdot(\Delta V)^2}{\Delta t} = \frac{0.5\times0.1\times10^{-6}\times5000^2}{600\times10^{-6}} \\ &= 2083\,\mathrm{W}. \end{aligned} \tag{11}$$

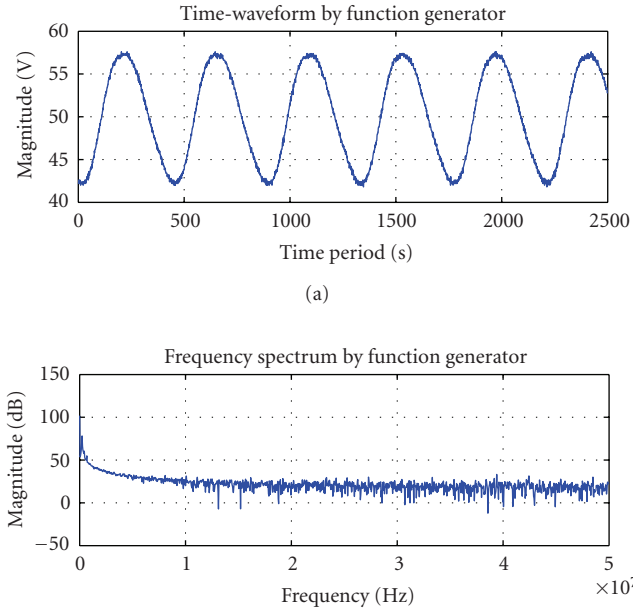

Figure 5: Output voltage across transformer.

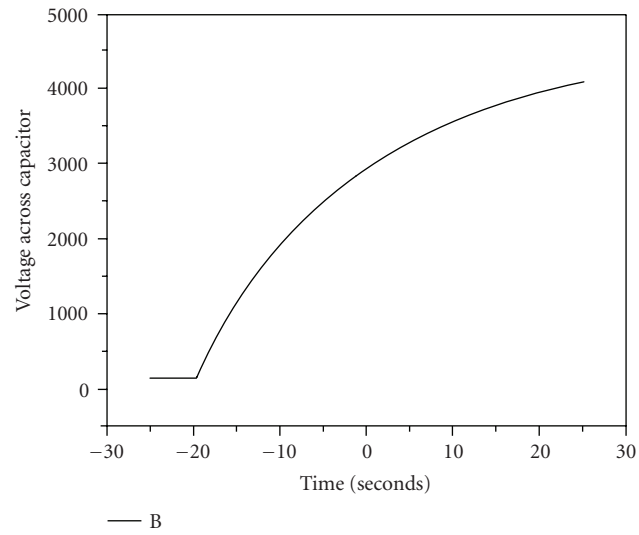

Figure 6: Waveform of capacitor charging.

The theoretical value of voltage is calculated by the following equation:

$$\begin{aligned} N_1 &= 15\ \text{turns}, \\ \mathrm{N}_2 &= N_1\frac{V_2}{V_1} = 15\frac{5000}{560} \approx 135\ \text{turns}, \\ N_1 &= 15\ \text{turns}, \\ \mathrm{V}_2 &= V_1\frac{N_2}{N_1} = 560\frac{135}{15} = 5040\ \text{volts}. \end{aligned} \tag{12}$$

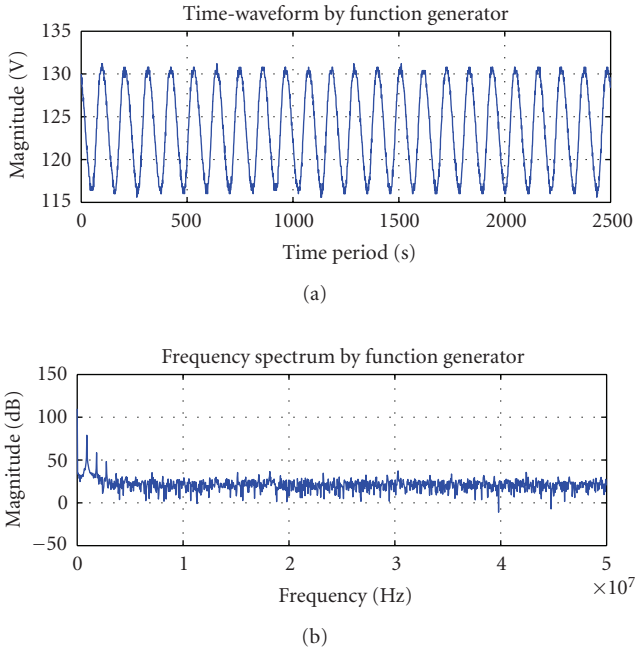

Figure 7: Transformer primary voltage with FFT.

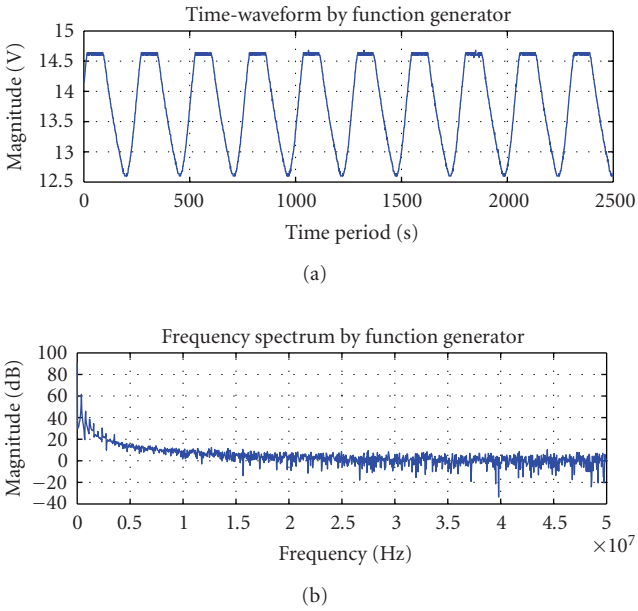

Figure 8: Output wave form of controller IC uc 3860.

The theoretical power value as per (11) is more than sufficient to ensure an actual value greater than the targeted 1.25 KW.

For approximate analysis using complex ac-circuit analysis [10–13] in this method, fundamental components of the waveforms are used for voltages and currents. This method cannot predict the various voltage and current waveforms appropriately, and the accuracy reduces as the switching frequency is away from resonance frequency (as in variable frequency-controlled converters) or as the duty ratio decreases (as in fixed frequency-controlled converters).

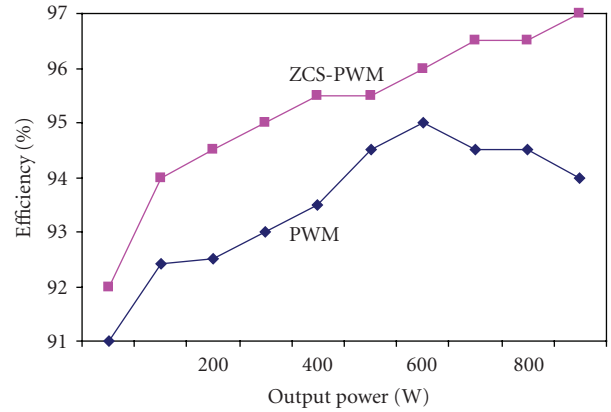

Figure 9: Comparison of efficiency of PWM and ZCS-PWM.

For Fourier series method or frequency domain approach [12, 13] method, all the predominant harmonics are taken into account. This method is simple and gives good results.

The output wave form is taken on the TPS2014 digital storage oscilloscope. The output voltage of transformer is as shown in Figure 5. The signal via digital storage oscilloscope (DSO) is analyzed in FFT toolbox of MATLAB. The commutation takes place at zero current; unwanted spikes and noise are present due to parasitic capacitance, PCB traces impendence, reverse recovery time of the antiparallel diodes, electromagnetic radiation, and coupling within the converter PCB. The noise signal can be seen from the fft wave form.

The charging voltage across the capacitor is shown in Figure 6. Figure 7 shows the input voltage to transformer. The output voltage across resonant controller UC3860 which drives the IGBT (IRG4PH40PUD) is shown in Figure 8. We can clearly see that the DC and first-order harmonic components are high [13]. The higher-order harmonic components are reduced very quickly [13]. The total harmonic distortion (THD) is small:

$$\text{THD} = \frac{V_{\text{ac}}}{V_{\text{fund}}} = \frac{\sqrt{\sum_{n=2}^{\infty} V_n^2}}{V_{\text{fund}}}. \tag{13}$$

The maximum peak reverses current flowing through the diode when one pair switch is open is −13 amps. The $I_{\text{ON max}}$ is 26 amps. From Figure 9, we can see that the efficiency of ZCS-PWM is much better [14] than that of ordinary PWM because the losses in the ZCS decrease due to soft switching.

6. CONCLUSION

With the new device technology recently developed, the performance of high-power converters can be improved dramatically in terms of dynamics, efficiency, size, and protection, due to the improved switching speed and the removal of the turn-off snubber. The series load resonant topology choice for the switching converter module resulted in minimized switching loss and reduced size of the heat

sink. The proposed schemes have several advantages over conventional scheme such as simple operation, easy analysis and control, and improved effiency.

REFERENCES

[1] J. Takesuye and S. Deuty, "Introduction to Insulated Gate Bipolar Transistors," Application Note AN1541/D, Motorola Inc, 1995.

[2] M. Trivedi and K. Shenai, "Internal dynamics of IGBT under zero-voltage and zero-current switching conditions," *IEEE Transactions on Electron Devices*, vol. 46, no. 6, pp. 1274–1282, 1999.

[3] A. C. Lippincott and R. M. Nelms, "A capacitor-charging power supply using a series-resonant topology, constant on-time/variable frequency control, and zero-current switching," *IEEE Transactions on Industrial Electronics*, vol. 38, no. 6, pp. 438–447, 1991.

[4] R. M. Nelms, B. E. Strickland, and M. Garbi, "High voltage capacitor charging power supplies for repetitive rate loads," in *Proceedings of IEEE Industry Applications Society Annual Meeting (IAS '90)*, vol. 2, pp. 1281–1285, Seattle, Wash, USA, October 1990.

[5] K. Okamura, H. Shimamura, N. Kobayashi, and K. Watanabe, "Development of a semiconductor switch for high power copper vapor lasers," in *Proceedings of the 11th IEEE International Pulsed Power Conference*, vol. 2, pp. 975–980, Baltimore, Md, USA, June-July 1997.

[6] J. Takesuye and S. Deuty, "Introduction to Insulated Gate Bipolar Transistors," Application Note AN1541/D, Motorola Inc, 1995.

[7] C. M. Liaw, S. J. Chiang, C. Y. Lai, K. H. Pan, G. C. Leu, and G. Hsu, "Modeling and controller design of current-mode controlled converter," *IEEE Transactions on Industrial Electronics*, vol. 41, no. 2, pp. 231–240, 1994.

[8] K. H. Liu, R. Oruganti, and F. C. Lee, "Resonant switches—topologies and characteristics," in *Proceedings of the 16th IEEE Annual Power Electronics Specialists Conference (PESC '85)*, pp. 106–116, Toulouse, France, June 1985.

[9] N. Mohan, T. M. Undeland, and W. P. Robbins, *Power Electronics: Converters, Applications and Design*, John Wiley & Sons, New York, NY, USA, 1989.

[10] R. L. Steigerwald, "A comparison of half-bridge resonant converter topologies," *IEEE Transactions on Power Electronics*, vol. 3, no. 2, pp. 174–182, 1988.

[11] O. P. Mandhana and R. G. Hoft, "Two-port characterization of DC to DC resonant converters," in *Procedings of the 5th IEEE Annual Applied Power Electronics Conference and Exhibition (APEC '90)*, pp. 737–745, Los Angeles, Calif, USA, March 1990.

[12] P. P. Roy, S. R. Doradla, and S. Deb, "Analysis of the series resonant converter using a frequency domain model," in *Proceedings of the 22nd IEEE Annual Power Electronics Specialists Conference (PESC '91)*, pp. 482–489, Boston, Mass, USA, June 1991.

[13] A. K. S. Bhat, "A generalized steady-state analysis of resonant converters using two-port model and Fourier-series approach," *IEEE Transactions on Power Electronics*, vol. 13, no. 1, pp. 142–151, 1998.

[14] C.-M. Wang, H.-J. Chiu, and D.-R. Chen, "Novel zero-current-switching (ZCS) PWM converters," *IEE Proceedings: Electric Power Applications*, vol. 152, no. 2, pp. 407–415, 2005.